01 Jan 2011

Femtosecond Laser Writing of Waveguides in Zinc Phosphate Glasses [Invited]

Luke B. Fletcher

Jon J. Witcher

Neil Troy

Signo Tadeu Dos Reis
Missouri University of Science and Technology, reis@mst.edu

et. al. For a complete list of authors, see https://scholarsmine.mst.edu/matsci_eng_facwork/18

Recommended Citation

L. B. Fletcher et al., "Femtosecond Laser Writing of Waveguides in Zinc Phosphate Glasses [Invited]," *Optical Materials Express*, Optical Society of America, Jan 2011.
The definitive version is available at https://doi.org/10.1364/OME.1.000845

Femtosecond laser writing of waveguides in zinc phosphate glasses [Invited]

Luke B. Fletcher, [1] Jonathan J. Witcher,[1] Neil Troy,[1] Signo T. Reis,[2] Richard K. Brow,[2] Rebeca Martinez Vazquez,[3] Roberto Osellame[3] and Denise M. Krol[1*]

[1]*Department of Applied Science, University of California Davis, Davis, California 95616, USA*
[2]*Department of Materials Science & Engineering, Missouri University of Science and Technology, Rolla, Missouri 65409, USA*
[3]Istituto di Fotonica e Nanotecnologie del CNR – Dipartimento di Fisica del Politecnico di Milano, *P.zza L. da Vinci 32, 20133 Milano, Italy*
**dmkrol@ucdavis.edu*

Abstract: We have studied the relationship between the initial glass composition and the structural changes associated with laser-induced refractive index modification in a series of Er-Yb doped and undoped zinc phosphate glasses. White light microscopy and waveguide experiments are used together with Raman and fluorescence spectroscopy to characterize the structural changes. The correlation between Raman peak shifts and fluorescence from phosphorus–oxygen hole center (POHC) defects indicates that fs-laser writing results in a depolymerization of the phosphate glass network. The results also show that the exact glass composition should be taken into account when fabricating waveguide devices in phosphate glasses, in order to both expand the fs-laser processing conditions and maximize favorable morphological changes for 3-D photonic devices.

OCIS codes: (320.2250) Femtosecond phenomena; (220.4000) Microstructure fabrication; (230.7370) Waveguides; (160.2750) Glass and other amorphous materials.

References and links

1. K. M. Davis, K. Miura, N. Sugimoto, and K. Hirao, "Writing waveguides in glass with a femtosecond laser," Opt. Lett. **21**(21), 1729–1731 (1996).
2. K. Miura, J. Qiu, H. Inouye, T. Mitsuyu, and K. Hirao, "Photowritten optical waveguides in various glasses with ultrashort pulse laser," Appl. Phys. Lett. **71**(23), 3329 (1997).
3. R. R. Gattass and E. Mazur, "Femtosecond laser micromachining in transparent materials," Nat. Photonics **2**(4), 219–225 (2008).
4. K. Itoh, W. Watanabe, S. Nolte, and C. Schaffer, "Ultrafast processes for bulk modification of transparent materials," MRS Bull. **31**(08), 620–625 (2006).
5. R. Osellame, G. Della Valle, N. Chiodo, S. Taccheo, P. Laporta, O. Svelto, and G. Cerullo, "Lasing in femtosecond laser written optical waveguides," Appl. Phys., A Mater. Sci. Process. **93**(1), 17–26 (2008).
6. M. J. Weber, "Science and technology of laser glass," J. Non-Cryst. Solids **123**(1-3), 208–222 (1990).
7. G. Della Valle, R. Osellame, and P. Laporta, "Micromachining of photonic devices by femtosecond laser pulses," J. Opt. A, Pure Appl. Opt. **11**(1), 013001 (2009).
8. M. Ams, G. D. Marshall, P. Dekker, M. Dubov, V. K. Mezentsev, I. Bennion, and M. J. Withford, "Investigation of ultrafast laser–photonic material interactions: Challenges for directly written glass photonics," IEEE J. Sel. Top. Quantum Electron. **14**(5), 1370–1381 (2008).
9. D. Esser, D. Mahlmann, D. Wortmann, and J. Gottmann, "Interference microscopy of femtosecond laser written waveguides in phosphate glass," Appl. Phys. B **96**(2-3), 453–457 (2009).
10. L. B. Fletcher, J. J. Witcher, W. B. Reichman, A. Arai, J. Bovatsek, and D. M. Krol, "Changes to the network structure of Er–Yb doped phosphate glass induced by femtosecond laser pulses," J. Appl. Phys. **106**(8), 083107 (2009).
11. R. Osellame, N. Chiodo, G. Della Valle, G. Cerullo, R. Ramponi, P. Laporta, A. Killi, U. Morgner, and O. Svelto, "Waveguide lasers in the C-band fabricated by laser inscription with a compact femtosecond oscillator," IEEE J. Sel. Top. Quantum Electron. **12**(2), 277–285 (2006).
12. R. Osellame, N. Chiodo, G. della Valle, S. Taccheo, R. Ramponi, G. Cerullo, A. Killi, U. Morgner, M. Lederer, and D. Kopf, "Optical waveguide writing with a diode-pumped femtosecond oscillator," Opt. Lett. **29**(16), 1900–1902 (2004).
13. A. Ferrer, A. Ruiz de la Cruz, D. Puerto, W. Gawelda, J. A. Vallés, M. A. Rebolledo, V. Berdejo, J. Siegel, and J. Solis, "In situ assessment and minimization of nonlinear propagation effects for femtosecond-laser waveguide writing in dielectrics," J. Opt. Soc. Am. B **27**(8), 1688 (2010).

#150726 - $15.00 USD Received 8 Jul 2011; revised 31 Jul 2011; accepted 1 Aug 2011; published 3 Aug 2011

14. L. B. Fletcher, J. J. Witcher, N. Troy, S. T. Reis, R. K. Brow, and D. M. Krol, "Direct femtosecond laser waveguide writing inside zinc phosphate glass," Opt. Express **19**(9), 7929–7936 (2011).
15. F. Liebau, M. O'Keefe, and A. Novrotsky, *Structure and Bonding in Crystals II* _Academic Press, New York, 1981, p. 197.
16. R. K. Brow, "Review: the structure of simple phosphate glasses," J. Non-Cryst. Solids **263–264**(1-2), 1–28 (2000).
17. A. K. Varshneya, *Fundamentals of inorganic glasses (2nd edition)*, Society of Glass Technology, Boston, MA (2006).
18. D. Ilieva, B. Jivov, G. Bogachev, C. Petkov, I. Penkov, and Y. Dimitriev, "Infrared and Raman spectra of Ga2O3–P2O5 glasses," J. Non-Cryst. Solids **283**(1-3), 195–202 (2001).
19. J. J. Hudgens, R. K. Brow, D. R. Tallant, and S. W. Martin, "Raman spectroscopy study of the structure of lithium and sodium ultraphosphate glasses," J. Non-Cryst. Solids **223**(1-2), 21–31 (1998).
20. R. Lebullenger, L. A. O. Nunes, and A. C. Hernandes, "Properties of glasses from fluoride to phosphate composition," J. Non-Cryst. Solids **284**(1-3), 55–60 (2001).
21. R. K. Brow, D. R. Tallant, S. T. Myers, and C. C. Phifer, "The Short Range Structure of Zinc Phosphate Glass," J. Non-Cryst. Solids **191**(1-2), 45–55 (1995).
22. L. B. Fletcher, J. J. Witcher, W. B. Reichman, A. Arai, J. Bovatsek, and D. M. Krol, "Changes to the network structure of Er-Yb doped phosphate glass induced by femtosecond laser pulses," J. Appl. Phys. **106**(8), 083107 (2009).
23. L. Popović, D. de Waal, and J. C. A. Boeyens, "Correlation between Raman wavenumbers and P—O bond lengths in crystalline inorganic phosphates," J. Raman Spectrosc. **36**, 2–11 (2005).
24. D. L. Griscom, E. J. Friebele, K. J. Long, and J. W. Fleming, "Fundamental defect centers in glass - electron-spin resonance and optical absorption studies of irradiated phosphorus-doped silica glass and optical fibers," J. Appl. Phys. **54**(7), 3743–3762 (1983).
25. D. Ehrt, P. Ebeling, and U. Natura, "UV transmission and radiation-induced defects in phosphate and fluoride-phosphate glasses," J. Non-Cryst. Solids **263-264**(1-2), 240–250 (2000).
26. U. Natura and D. Ehrt, "Modeling of excimer laser radiation induced defect generation in fluoride phosphate glasses," Nucl. Instrum. Methods Phys. Res. B **174**(1-2), 151–158 (2001).
27. U. Natura and D. Ehrt, "Generation and healing behavior of radiation-induced optical absorption in fluoride phosphate glasses: the dependence on UV radiation sources and temperature," Nucl. Instrum. Methods Phys. Res. B **174**(1-2), 143–150 (2001).
28. J. W. Chan, T. Huser, J. S. Hayden, S. H. Risbud, and D. M. Krol, "Fluorescence spectroscopy of color centers generated in phosphate glasses after exposure to femtosecond laser pulses," J. Am. Ceram. Soc. **85**(5), 1037–1040 (2002).

1. Introduction

Femtosecond laser micromachining of glass can be used inside a variety of active glasses to fabricate waveguide lasers and amplifiers, with applications in three-dimensional photonic circuits [1–7]. Phosphate glasses are important substrates for active devices because they can incorporate high concentrations of rare-earth ions. However, many phosphate glasses, such as the commercially available Schott IOG-1 or Kigre QX and MM-2a glasses, exhibit complex refractive index profiles that can be used for waveguiding only when very specific combinations of laser processing parameters are used [7–13]. This makes the fabrication of high quality single-mode waveguides more difficult.

While it is possible, in some phosphate glasses, to vary the writing techniques in order to achieve positive changes to the refractive index, the effect of varying the glass composition has not been investigated to the same degree. We have recently demonstrated that in zinc phosphate glasses the initial composition plays an important role in determining the structural changes that result from fs-laser modification [14]. We found that in a series of zinc polyphosphate glasses only the glass with composition $60ZnO\text{-}40P_2O_5$ exhibited localized positive refractive index changes that can be used to fabricate optical waveguide devices with direct single scan femtosecond laser waveguide writing techniques.

In this paper, we report the fundamental relationships between the initial composition of doped and undoped zinc phosphate glasses and the structural changes associated with refractive index modification that result from fs-laser irradiation. Changes in glass structure have been studied using scanning confocal micro-Raman and fluorescence microscopy. Systematic changes in the Raman spectrum and the excited photoluminescence indicate atomic level changes to the phosphate network that depend on the femtosecond laser writing conditions and initial phosphate glass composition.

#150726 - $15.00 USD Received 8 Jul 2011; revised 31 Jul 2011; accepted 1 Aug 2011; published 3 Aug 2011

2. Background on phosphate glasses

2.1 Glass structure

The structure of phosphate glasses can be described as a network of phosphate tetrahedra that are linked through covalent bonding of corner shared oxygen atoms, referred to as bridging oxygen atoms. Oxygen atoms that do not link two phosphate tetrahedra are called non-bridging; the ratio of bridging to non-bridging oxygens depends on glass composition. Phosphate glasses typically consist of long "polymer like" phosphate chains. The linked phosphate tetrahedra have one, two, three, or four non-bridging oxygens. These units can be classified using Q^i terminology [15,16], where i represents the number of bridging oxygen atoms per tetrahedron (Fig. 1). For example, a Q^2 tetrahedron links to two others through bridging oxygens in a phosphate chain anion, with Q^1 tetrahedra terminating the ends of the chains. The role of network modifying oxides in the glass is to break up or depolymerize the phosphate chains as the [O]/[P] ratio increases [17]. The phosphate chain and ring anions are linked by bonds between various modifying metal cations and the non-bridging oxygen; these bonds are more ionic in nature.

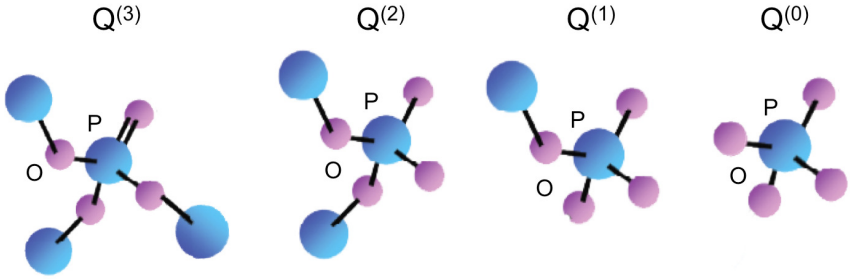

Fig. 1. Phosphate tetrahedral units – oxygen atoms (pink) connected to a phosphorus atoms (blue); Q^3 crosslinking units; Q^2 middle units; Q^1 end units; Q^0 isolated units.

2.2 Raman spectroscopy

Raman spectroscopy has been used to study the structures of phosphate glasses [16,18–21]. Figure 2 shows the Raman spectrum for a commercial metaphosphate glass.

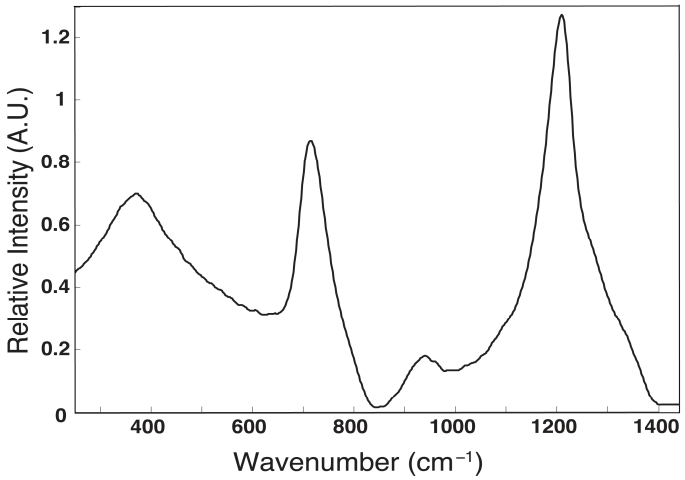

Fig. 2. Raman spectrum of commercial phosphate glass (MM-2a60 from Kigre Inc.)

The broad Raman band between 200 cm^{-1} and 600 cm^{-1} is due to internal deformation bending modes of phosphate chains, both in-chain PO_2 and OPO bending. The large band

#150726 - $15.00 USD Received 8 Jul 2011; revised 31 Jul 2011; accepted 1 Aug 2011; published 3 Aug 2011

around 710 cm^{-1} is due to the symmetric stretching mode of bridging oxygen between two Q^2 tetrahedra, $(POP)_{sym}$. The small band at 940 cm^{-1} is assigned to the asymmetric stretching mode, $(POP)_{asym}$. The large band at 1209 cm^{-1} is due to the symmetric stretching of the P–O non-bridging oxygens on Q^2 phosphate tetrahedra, $(PO_2)_{sym}$. The 1300 cm^{-1} peak, a shoulder of the 1209 cm^{-1} peak, is the asymmetric stretching of P–O non-bridging oxygen atoms, $(PO_2)_{asym}$. For this glass composition, with a nominal [O]/[P] ratio of 3, long metaphosphate chains dominated by Q^2 tetrahedra are expected, consistent with the Raman spectrum shown.

2.3 fs-laser modification

Previous studies [14,22] have shown that fs laser writing in phosphate glasses results in structural changes that can be detected as slight deviations in the vibrational spectrum measured using Raman spectroscopy. The exact peak position of several of the Raman bands, in particular the 1209 cm^{-1} band, has been shown to be very sensitive to small changes in network structure. Systematic shifts in this Raman peak to higher and lower wavenumbers indicate a decrease and/or increase in the P-O network bond length resulting in an overall expansion and/or contraction of the phosphate network [22].

Using a Rinck Electronik 2-D refractive index profilometer, we have been able to directly measure changes to the index of refraction spatially (Fig. 3(b)) on the fs-laser modified Er-Yb doped phosphate glass sample, and examine the relationship to changes in the 1209 cm^{-1} Raman mode (Fig. 3(a)). The differences in refractive index within the heat effected area (neglecting the stress induced changes directly surrounding the modification) are shown to correlate spatially with the 1209 cm^{-1} Raman signal shifts, where both the direction and magnitude of the Raman shifts correlate with the changes in refractive index (Fig. 3(c)).

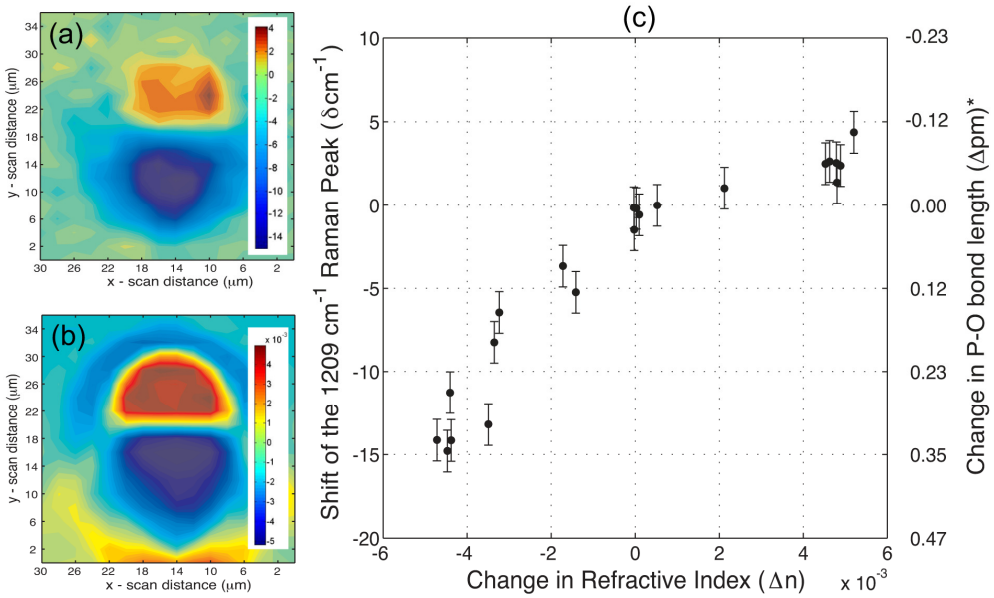

Fig. 3. Fs-laser modified Er-Yb doped phosphate glass written with 885 kHz rep rate, 320 nJ pulse energy, 50 μm/s scan speed. (a) Color map of shifts in the relative spectral position of the 1209 cm^{-1} Raman peak as a function of the spatial position (b) Color map of changes in the refractive index as a function of the spatial position (c) Plot of the shifts in the 1209 cm^{-1} Raman peak as a function of the change in refractive index for the heat effected area. *Calculated change in P-O bond length [23].

#150726 - $15.00 USD Received 8 Jul 2011; revised 31 Jul 2011; accepted 1 Aug 2011; published 3 Aug 2011

2.4 Fluorescence spectroscopy

Radiation induced defects have been extensively studied in phosphate and phosphorus containing glasses over the last couple of decades of materials research [24–27]. Several color center species are believed to result from exposure to high-energy electromagnetic radiation (UV, X-rays, gamma rays). The POHC (Phosphorus Oxygen Hole Center) is characterized by an unpaired electron shared between two orbitals of two non-bridging oxygens bound to a phosphorus atom (Fig. 4(c)). Other defects such as the PO_3^{2-} (phosphoryl), PO_4^{4-} (phosphoranyl), PO_2^{2-} (phosphinyl), are also responsible for induced defect absorption bands found in various phosphate glass systems. These defects absorb at high optical energies from 4.6 to 5.9 eV. The stable POHC defect has very large absorption bands at 2.2, 2.5, and 5.3 eV.

Results from previous experiments show that, after modifying IOG-1 glass with fs-pulses, a fluorescence band centered at roughly 600 nm can be observed (Fig. 4(b) using 488 nm as an excitation source [28]). This emission band has been characterized as a POHC defect. The assignment is supported by a comparison of the structural similarities in the atomic arrangements between the POHC defect and the equivalent Non-Bridging Oxygen Hole Centers (NBHOC) in fused silica [28]. The peaks at 590 nm, 615 nm, 640 nm and 665 nm are artifacts of the transmission profile from a 488 nm dichroic filter that was used in the experimental setup. The POHC defect fluorescence is indicative of a damage and possible depolymerization of the phosphate network as a result of laser irradiation.

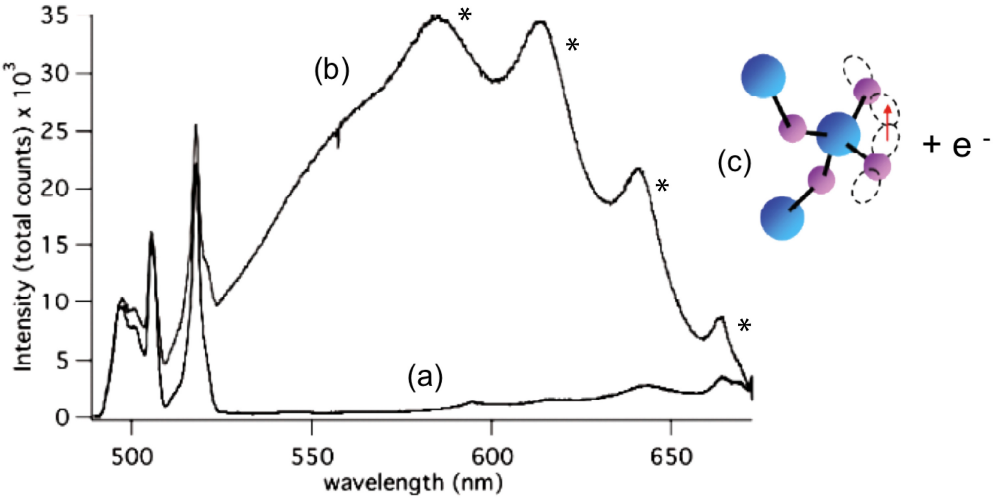

Fig. 4. (a) spectra of unmodified IOG-1 (Schott Inc) phosphate glass; (b) spectra of fs-modified IOG-1 phosphate glass; (c) POHC defects: a hole gets trapped on two orbitals of two oxygen atoms [24,28]. *Artifacts from a 488 nm dichroic filter.

3. Experimental Setup and Procedures

3.1 Material preparation

Various undoped and rare-earth doped zinc phospate glasses, with nominal compositions as shown in Table 1, were prepared. Reagent grade ZnO (zinc oxide), $NH_4H_2PO_4$ (ammonium phosphate), $Al(PO_3)_3$ (aluminum phosphate), Er_2O_3 (erbium oxide) and Yb_2O_3 (ytterbium oxide) were used as raw materials. Two Er/Yb-doped glasses were prepared from the $60.0ZnO\text{-}40.0P_2O_5$ base glass. For one composition, Er_2O_3 and Yb_2O_3 was substituted for ZnO and P_2O_5 was increased to retain a constant [O]/[P] ratio (glass 5 in Table 1) and for the second, the rare earth oxides were added directly to the base glass so that the nominal [O]/[P] ratio increased, from 3.25 to 3.33 (glass 6 in Table 1). For each composition the appropriate raw materials were thoroughly mixed and calcined at 500°C for 12 hours. The batches were

#150726 - $15.00 USD Received 8 Jul 2011; revised 31 Jul 2011; accepted 1 Aug 2011; published 3 Aug 2011

then melted in alumina crucibles at 1000°C for two hours and rapidly quenched. The resulting glass frit was ground into a powder and remelted in a Pt crucible for one hour at 1050°C into a homogeneous melt. The melts were poured into steel molds, cooled and subsequently annealed for 2 hours near T_g. The samples, which were 10mm x 5mm x 5mm in size, were polished using SiC paper and diamond pastes to a finish of 0.25 microns. The actual compositions of the glasses were not determined. However, as discussed below, their respective Raman spectra indicate that the actual compositions are similar to the nominal compositions, and so the latter will be used throughout this report.

Table 1. Phosphate glass properties

Sample	Composition (mole%)	[O]/[P]	Density (g/cm^3) +/–.005 g/cm^3	Refractive Index (632 nm) +/– 0.001	T_g (C°) +/– 2°C
1	$10.0Al_2O_3$-30.0ZnO-$60.0P_2O_5$	***3.00***	2.71	1.522	393
2	$50.0ZnO$-$50.0P_2O_5$	***3.00***	2.88	1.521	451
3	$55.0ZnO$-$45.0P_2O_5$	***3.11***	3.06	1.545	425
4	$60.0ZnO$-$40.0P_2O_5$	***3.25***	3.29	1.576	416
5	$0.7Er_2O_3$-$1.3Yb_2O_3$-$56.0ZnO$-$42.0P_2O_5$	***3.25***	3.31	1.577	446
6	$0.7Er_2O_3$-$1.3Yb_2O_3$-$58.8ZnO$-$39.2P_2O_5$	***3.33***	3.26	1.575	425
7	$65.0ZnO$-$35.0P_2O_5$	***3.43***	3.52	1.604	446

3.2 Optical experiments

All of the optical experiments, including fs-laser waveguide writing inside a variety of phosphate glasses, characterizing the changes to the glass network at the microscopic-level, as well as Raman and fluorescence microscopy, were performed with the integrated set-up shown in Fig. 5.

Waveguide writing experiments were performed with a 1 kHz, regeneratively amplified, Ti:Sapphire femtosecond laser system (Spectra Physics Merlin-Spitfire). The glass sample was sitting on a computer controlled motorized 3-d (x,y,z) translation stage, with an adjustable 6-d (x,y,z,θ,ϕ,δ) platform, which the sample was secured on, for fine tuning and alignment purposes. The sample was illuminated from the back by a white light source and imaged onto a CCD camera through the dichroic mirror. After the ultrafast laser beam was focused into the sample, the sample was translated along the desired direction and afterwards the micromachined features/patterns were viewed with the CCD camera. The experiments were performed using the longitudinal writing setup; Adjustments to the fs-laser power were made using a half wave plate and a polarizing beam splitter placed at the output of the regenerative amplifier.

White light images of the modified areas were collected both perpendicular to, and normal to, the fs-laser beam propagation direction, under most experiments, using a 20x (0.40 NA) objective and a CCD camera. A 10x (0.21 NA) objective was used to focus 660 nm laser light into the input waveguide facet, and a 10x (0.20 NA) objective was focused at the output facet in order to characterize the guiding properties. Mode profiles of the transmitted 660 nm laser light were obtained by imaging the near-field intensity at the output facet of the waveguide using a CCD camera.

#150726 - $15.00 USD Received 8 Jul 2011; revised 31 Jul 2011; accepted 1 Aug 2011; published 3 Aug 2011

Spectroscopy was performed on the fs-laser induced modifications using an adjustable power 473 nm cw laser after waveguides/modifications were written. The 473 nm excitation beam was directed through a high NA focusing objective using a 50/50 broadband dichroic beam splitter and focused into the glass sample. Backscatter signals produced by the 473 nm laser excitation were collected by the same objective and directed through the 50/50 beam splitter. A 50 μm diameter pinhole was used to ensure Raman signals were only collected from the focal volume of the objective. An Oriel 500 spectrometer in conjunction with a CCD camera (LN-CCD Princeton Instruments) was used to collect spectral signals that passed through the pinhole setup. The spectrometer was used with a 1200 grooves/mm grating centered at 500 nm to collect Raman signals, and a 600 grooves/mm grating centered at 620 nm to collect fluorescence signals.

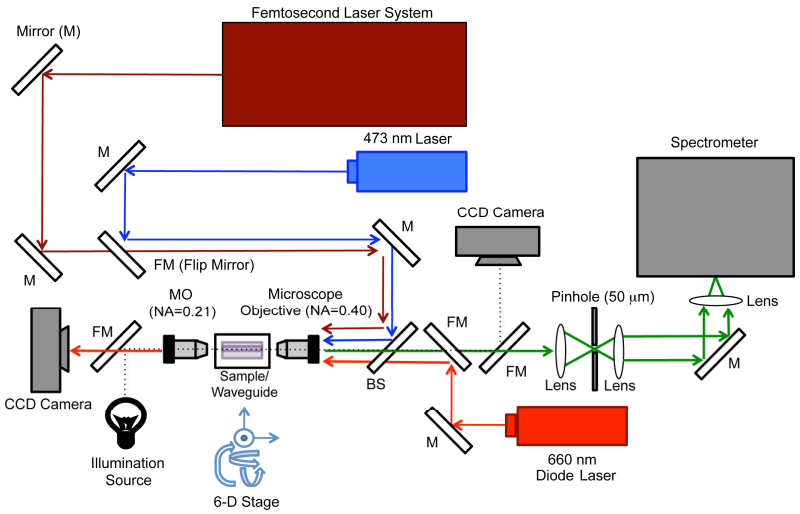

Fig. 5. Diagram of fully integrated free-space all-optical system used for (a) femtosecond laser waveguide writing inside phosphate glass; (b) in situ confocal fluorescence and Raman microscopy; (c) in situ white light microscopy and waveguide characterization.

4. Results and Discussion

4.1 Waveguide properties

Figures 6a and b show white light microscope images of fs-laser written lines created in the different zinc phosphate glasses. Figure 6c shows the near field images of the waveguide output in the respective glasses. The images in Figs. 6 (a-b) reveal that the morphology of the lines is rough for most of the glasses, except for the 60.0ZnO-40.0P_2O_5, 65.0ZnO-35.0P_2O_5, 0.75Er_2O_3-1.3Yb_2O_3-56.0ZnO-42.0P_2O_5, and the 0.7Er_2O_3-1.3Yb_2O_3-58.8ZnO-39.2P_2O_5 glass. Of these compositions only the 60.0ZnO-40.0P_2O_5 and the 0.7Er_2O_3-1.3Yb_2O_3-56.1ZnO-42.0P_2O_5 glass exhibited good waveguiding behavior (Fig. 6c). This indicates that in these two glasses the induced refractive index changes in the focal region of the fs-laser are positive whereas for the other compositions these changes are negative. The obvious differences in response to fs-laser exposure of these glasses compared to that of the other zinc phosphate glass compositions, indicate that the initial phosphate glass composition (or structure) plays an important role in producing high quality waveguides. Specifically, the different results for the 0.7Er_2O_3-1.3Yb_2O_3-56.0ZnO-42.0P_2O_5 and the 0.7Er_2O_3-1.3Yb_2O_3-58.8ZnO-39.2P_2O_5 glass demonstrate a sensitivity to very small changes in bulk glass composition.

#150726 - $15.00 USD Received 8 Jul 2011; revised 31 Jul 2011; accepted 1 Aug 2011; published 3 Aug 2011

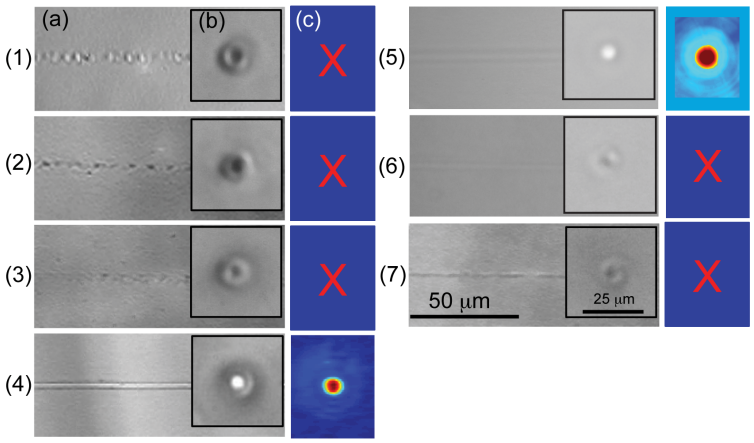

Fig. 6. Microscope images of fs-modified zinc phosphate glass written with fs-laser fluences of 8 J/cm^2 (1) 30.0ZnO-10.0Al2O3-60.0P2O5 glass (2) 50.0ZnO-50.0P_2O_5 glass (3) 55.0ZnO-45.0P_2O_5 glass (4) 60.0ZnO-40.0P_2O_5 glass (5) 0.7Er_2O_3-1.3Yb_2O_3-56.0ZnO-42.0P_2O_5 glass (6) 0.7Er_2O_3-1.3Yb_2O_3-58.8ZnO-39.2P_2O_5 glass (7) 65.0ZnO-35.0P_2O_5 glass; (a) white light images of the modification along the waveguide direction (b) Transmission white light images of the modification cross-section (c) 660 nm transmission near field images.

4.2 Confocal Raman microscopy

Figure 7 shows the Raman spectra for the different zinc phosphate glasses prior to fs-laser irradiation. The spectra, which are similar to the spectrum shown in Fig. 2, reveal systematic changes in the phosphate structural network with changes in composition.

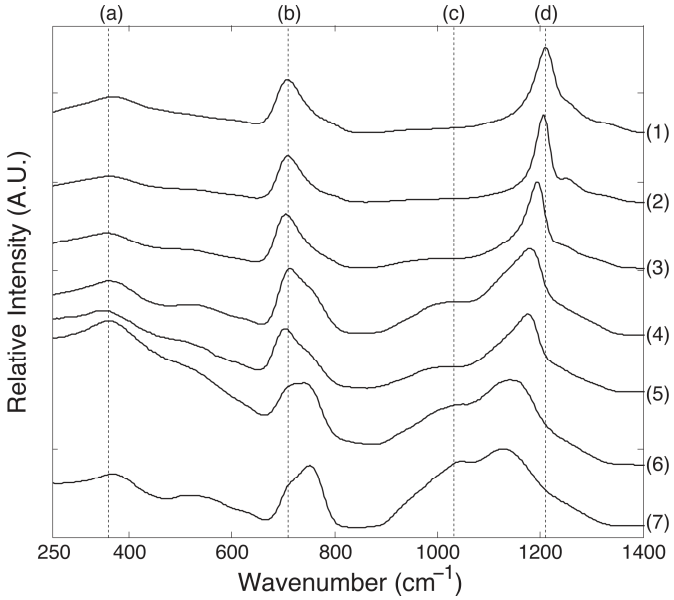

Fig. 7. Raman spectra of unmodified bulk phosphate glasses (1) 30.0ZnO-10.0Al_2O_3-60.0P_2O_5 glass (2) 50.0ZnO-50.0P_2O_5 glass (3) 55.0ZnO-45.0P_2O_5 glass (4) 60.0ZnO-40.0P_2O_5 glass (5) 0.7Er_2O_3-1.3Yb_2O_3-56.0ZnO-42.0P_2O_5 glass (6) 0.7Er_2O_3-1.3Yb_2O_3-58.8ZnO-39.2P_2O_5 glass (7) 65.0ZnO-35.0P_2O_5 glass; (a) in chain PO_2 and OPO bending (b) (POP) symmetric stretch (bridging oxygen), Q^2 species (c) P-O stretch, Q^1 chain terminator (d) (PO_2) symmetric stretch (non-bridging oxygen), Q^2 species.

With an increase in the [O]/[P] ratio the 1030 cm^{-1} peak intensity (Q^1 tetrahedra – non-bridging symmetric stretching vibrations that discontinue the metaphosphate chain) increases

#150726 - $15.00 USD Received 8 Jul 2011; revised 31 Jul 2011; accepted 1 Aug 2011; published 3 Aug 2011

while the 1209 cm^{-1} peak (indicative of Q^2 tetrahedra) decreases and shifts towards lower wavenumbers, consistent with the fact that Q^2 tetrahedra that form long chains in metaphosphate glasses ([O]/[P] = 3.0) are replaced by Q^1 tetrahedra that terminate progressively shorter chains in the polyphosphate compositions. In addition, the Raman band near 700 cm^{-1} for glasses with nominal [O]/[P] = 3, associated with the symmetric P-O-P stretching modes of bridging oxygens between Q^2 tetrahedra, develops a second peak near 750 cm^{-1} that is associated with the symmetric P-O-P stretching modes of bridging oxygens that link at least one Q^1 tetrahedra, as the nominal [O]/[P] ratio increases. The compositional dependences of the Raman spectra indicate that the actual compositions of these glasses vary as expected from their nominal compositions.

In order to monitor the atomic scale structural changes resulting from fs-laser writing, confocal Raman and fluorescence experiments were performed on all fs-laser modified glass samples. Systematic changes in the Raman spectra were observed, both as a function of composition and fs-laser fluence. Raman peak positions were determined in two ways; 1) the wavenumber for which the maximum number of counts was detected and 2) the peak position determined from fitting the peak to a Gaussian curve. Both procedures yielded the same value for the peak position. For glasses where no favorable waveguiding structures could be fabricated, the 1209 cm^{-1} Raman peak associated with P-O bonds on Q^2 tetrahedra showed a consistent shift to lower wavenumbers in the modified regions. The spatial dependence of the shift was measured by carefully scanning over the modified cross-section in 1.5 μm step sizes [14]. The magnitude of the maximum shift not only varied from sample to sample but it also depended on the amount of fs-laser energy deposited into the glass (see section 4.4).

For the two glasses that showed good guiding no shift of the $(PO_2)_{sym}$ Raman peak could be observed within the modified area for any fs-laser fluences used. Apparently the structure of these glasses, both with [O]/[P] = 3.25, was not changed in the same way as those with lower ZnO contents. For the 65.0ZnO-35.0P_2O_5 glass the peak at 1209 cm^{-1} could not be distinguished in the Raman spectrum, due to the fact that this glass has a relatively low concentration of Q^2 tetrahedra (about 15%).

It is important to note the overall similarities that exist between the Raman spectrum of the 60.0ZnO-40.0P_2O_5 bulk glass (Fig. 7(4)) and the spectrum of the 0.7Er_2O_3-1.3Yb_2O_3-56.0ZnO-42.0P_2O_5 bulk glass sample (Fig. 7(5)). The nominal [O]/[P] ratios of both glasses are the same and Raman spectra indicate that the two glasses have similar phosphate anions constituting their structures. On the other hand, when erbium oxide and ytterbium oxide are added directly to the 60.0ZnO-40.0P_2O_5 glass, the nominal [O]/[P] ratio increases (glass 6, Table 1) and this is reflected in the Raman spectrum (Fig. 7(6)) which indicates a greater degree of depolymerization of the phosphate network, forming shorter chains, and a bulk phosphate structure (i.e. Raman signature) that resembles the 65.0ZnO-35.0P_2O_5 glass composition (Fig. 7(7)).

4.3 Confocal fluorescence microscopy

Fluorescence spectra were measured for the undoped fs-laser modified zinc phosphate glasses. The Er-Yb doped glasses were not included in this study because the fluorescence spectrum was complicated by signals due to the Er^{3+} transitions. However, no observable luminescence was recorded within the emissions range of POHC defects. The spectra for laser-modified 30.0ZnO-10.0Al_2O_3-60.0P_2O_5 glass in Fig. 8 show a broad photoluminescence band centered at 630 nm within the modified volume. This fluorescence peak is caused by fs-laser induced POHC (phosphorus-oxygen-hole-center) defects. The fluorescence peak intensity increases with increasing fs-laser fluence indicating that the concentration of POHC defects inside the laser-modified 30.0ZnO-10.0Al_2O_3-60.0P_2O_5 glass depends on the amount of fs-laser energy that is deposited into the glass.

The overall fluorescence intensity, and thus the concentration of the induced POHC defects, however, is not the same for every glass composition used in this experiment. This can be observed by measuring this fluorescence as a function of changing glass composition.

#150726 - $15.00 USD Received 8 Jul 2011; revised 31 Jul 2011; accepted 1 Aug 2011; published 3 Aug 2011

As the results in Fig. 9 show, the defect fluorescence depends on both the initial glass composition and the amount of fs-laser energy deposited into the glass. Figure 9 clearly shows how both variables (glass composition and fs-laser fluence) have an effect on the intensity of the POHC fluorescence, and so on the susceptibility of the glass to network damage. Glasses with higher [O]/[P] ratios have less network damage after fs-modification. More importantly, the glass compositions with an [O]/[P] > 3.25 demonstrate no observable POHC defects, even after modification with fs-laser fluencies >40 J/cm^2.

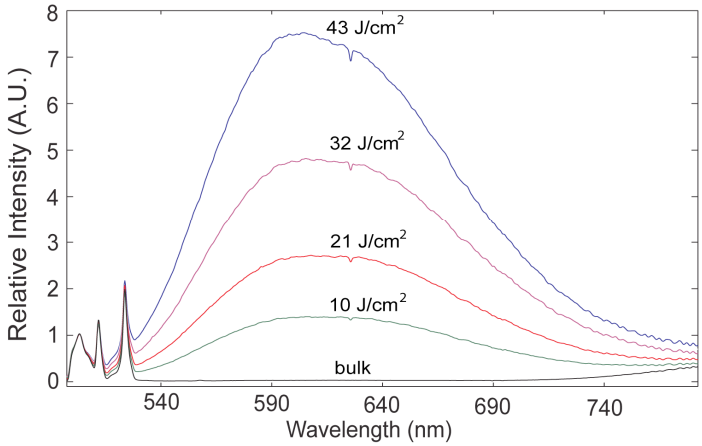

Fig. 8. Fluorescence spectra of laser-modified and bulk 30.0ZnO-10.0Al_2O_3-60.0P_2O_5 glass for various fs-laser fluences.

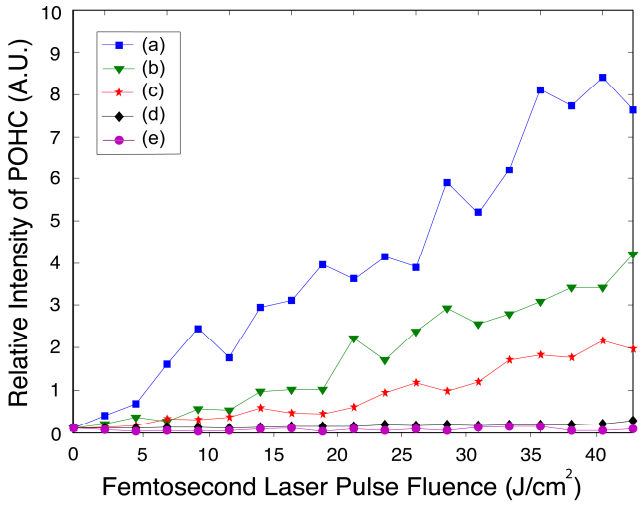

Fig. 9. Change in intensity of POHC fluorescence as a function of changing fs-laser pulse fluence for various glass compositions of (a) 30.0ZnO-10.0Al_2O_3-60.0P_2O_5 glass (b) 50.0ZnO-50.0P_2O_5 glass (c) 55.0ZnO-45.0P_2O_5 glass (d) 60.0ZnO-40.0P_2O_5 glass (e) 65.0ZnO-35.0P_2O_5.

4.4 POHC fluorescence and Raman signal shift

Upon further analysis of the data it is clear that the measured POHC fluorescence correlates with the spectral position of the 1209 cm^{-1} Raman signal. Figure 10 shows that glasses with greater fluorescence intensities from laser modified regions possess greater shifts in the $(PO_2)_{sym}$ Raman peak frequency. This is consistent with a picture in which the deposition of fs-laser energy results in significant expansion and damage to the glass network, producing a

#150726 - $15.00 USD Received 8 Jul 2011; revised 31 Jul 2011; accepted 1 Aug 2011; published 3 Aug 2011

material with POHC defects (broken P-O bonds) and a lower glass density (longer P-O bond length). It also shows the distinctly different response of glasses with [O]/[P] ratios > ~3.2. For these glasses no significant POHC fluorescence or significant Raman shifts were observed even with pulse fluences up to 40 J/cm^2.

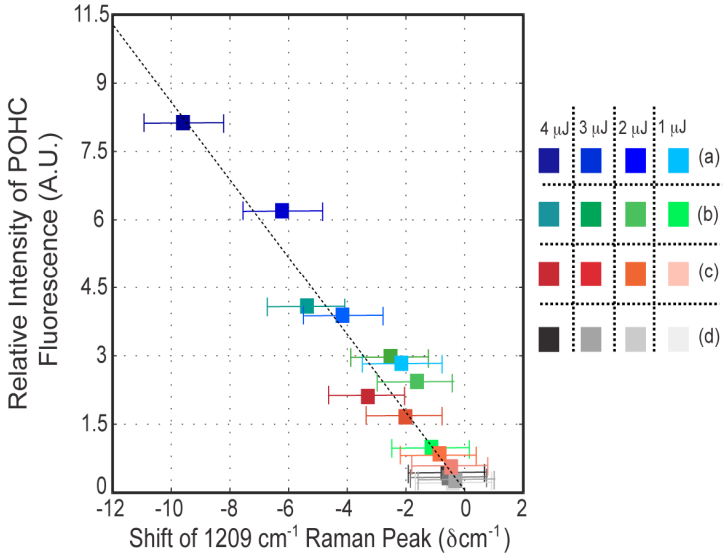

Fig. 10. Maximum change in intensity of POHC fluorescence as a function of the maximum 1209 cm^{-1} Raman mode shift modified with changing fs-laser pulse energy for various glass compositions of (a) 30.0ZnO-10.0Al_2O_3-60.0P_2O_5 glass (b) 50.0ZnO-50.0P_2O_5 glass (c) 55.0ZnO-45.0P_2O_5 glass (d) 60.0ZnO-40.0P_2O_5 glass..

A comparison of the seven zinc phosphate glass samples and their respective material properties, listed in Table 1, shows that these glasses have very similar overall glass properties. However, a closer examination of the data reveals that the two zinc phosphate glasses that resulted in positive changes to the refractive index after fs-laser modification (samples 4 and 5) can only be distinguished from the other glass substrates by their initial phosphate structure ([O]/[P] ratio). While samples 4 and 5 have slightly different overall material properties, the key link between these two samples is their initial phosphate structure. The results from Table 1 in combination with the Raman data in Fig. 7 indicate that the initial zinc phosphate glass structure plays a very important role in the resulting change to refractive index after fs-laser irradiation. It is a key property and fundamental parameter that can be used to predict how the glass will respond to the absorption of tightly focused fs-laser pulses.

Acknowledgement

The authors acknowledge financial support through NSF Grant Nos. DMR-0305202, NSF-DMR 0801786 and NSF-CMMI 0825572.

#150726 - $15.00 USD Received 8 Jul 2011; revised 31 Jul 2011; accepted 1 Aug 2011; published 3 Aug 2011